

SYNCHRONIZATION AND HOPF BIFURCATION IN STUART–LANDAU NETWORKS

KUAN-WEI CHEN¹ AND TING-YANG HSIAO²

ABSTRACT. The Kuramoto model has shaped our understanding of synchronization in complex systems, yet its phase-only formulation neglects amplitude dynamics that are intrinsic to many oscillatory networks. In this work, we revisit Kuramoto-type synchronization through networks of Stuart–Landau oscillators, which arise as the universal normal form near a Hopf bifurcation. For identical natural frequencies, we analyze synchronization in two complementary regimes. Away from criticality, we establish topology-robust complete synchronization for general connected networks under explicit sufficient conditions that preclude amplitude death. At criticality, we exploit network symmetries to analyze the onset of collective oscillations via Hopf bifurcation theory, demonstrating the emergence of synchronized periodic states in ring-symmetric networks. Our results clarify how amplitude dynamics enrich the structure of synchronized states and provide a bridge between classical Kuramoto synchronization and amplitude-inclusive models in complex networks.

1. INTRODUCTION

Over the past fifty years, the Kuramoto model [1, 2] has played a central role in the study of synchronization, serving not only as a prototypical mathematical model but also as a conceptual framework for understanding collective dynamics in large populations of interacting oscillators. Its influence extends across disciplines ranging from physics [3, 4, 5, 6], applied mathematics [7, 8, 9, 10, 11, 12], neuroscience, biology [13, 14, 15, 16], to network science [17, 18, 19, 20, 21, 22], and non-Abelian and operator-valued extensions [23, 24, 25, 26]. Beyond its specific formulation, the Kuramoto paradigm has shaped our intuition about how coherence emerges from simple coupling rules, and it continues to inform how synchronization phenomena are modeled and interpreted in complex systems. We refer interested readers to [27, 28] for a comprehensive overview.

Beyond serving as a specific mathematical model, the framework of Kuramoto oscillators has come to define how synchronization itself is conceptualized in networked systems. But even under the most classical assumptions, a complete characterization of synchronized states has only been achieved relatively recently. Recent work by Hsiao–Lo–Zhu [7, 8] has demonstrated that, within the classical Kuramoto

¹ (CORRESPONDING AUTHOR) MEIJI INSTITUTE FOR ADVANCED STUDY OF MATHEMATICAL SCIENCES, MEIJI UNIVERSITY, 4-21-1 NAKANO, NAKANO-KU, TOKYO 164-8525, JAPAN.

² (CORRESPONDING AUTHOR) INTERNATIONAL SCHOOL FOR ADVANCED STUDIES (SISSA), VIA BONOMEA 265, 34136, TRIESTE, ITALY.

E-mail addresses: ¹kwchen0613@meiji.ac.jp, ²thsiao@sissa.it.

Date: January 16, 2026.

Key words and phrases. synchronization; Kuramoto model; Stuart–Landau oscillators; complex networks; Hopf bifurcation.

model, various notions of synchronization are in fact equivalent. In particular, under the standard Kuramoto setting, synchronization cannot be generated by periodic orbits; instead, synchronization necessarily emerges through phase locking. For the case of identical natural frequencies, we refer the reader to the comprehensive discussion in [29, 30]. Historically, over the past decades, synchronization has often been implicitly identified with phase alignment, a viewpoint that has proven remarkably successful in explaining collective behavior across a wide range of applications. However, recent developments across multiple disciplines have highlighted that synchronization cannot be reduced to phase coherence alone [31, 32, 25, 6, 3]. In particular, finite-time blow-up phenomena reveal the essential distinction between generalized phases [3] and classical phases [1, 2]. This broader perspective calls into question the extent to which classical phase-only descriptions capture the full structure of synchronized states. If one aims to capture a wider range of alignment mechanisms observed in real oscillatory systems—such as amplitude synchronization—it becomes necessary to return to a more fundamental level of description. From this perspective, networks of Stuart–Landau oscillators [33, 34, 35, 36] provide a natural setting in which the foundations of Kuramoto-type synchronization can be revisited; see also [21, 22, 17] for modern treatments. For the case of non-identical coupling strengths, please refer to Chen–Shih [17]. Finally, we remark that under certain structural and dynamical assumptions, the Stuart–Landau system can be reduced to a pure phase dynamics. The earliest systematic studies along this direction can be traced back to the work of Aronson–Ermentrout–Kopell [37]. More recent and modern treatments of phase reduction can be found, for example, in Nakao [38] and Bick–Böhle–Kuehn [39].

In this work, we focus on networks of Stuart–Landau oscillators with identical natural frequencies and investigate synchronization across general network topologies. Our analysis reveals that a single synchronized oscillatory state admits complementary mathematical descriptions, depending on the network structure and parameter regime. The two approaches provide complementary descriptions of the same synchronized state: the first establishes its robustness across general network topologies, while the second resolves its onset and modal structure in highly symmetric networks at criticality $\mu = 0$. In Section 3, we consider general connected network topologies and study synchronization away from criticality. We first characterize sufficient conditions that prevent amplitude death, and then show that oscillator amplitudes asymptotically align, leading the system toward complete synchronization. In Section 4, we turn to the critical regime and examine synchronization through the lens of Hopf bifurcation. While the synchronized dynamics of two coupled Stuart–Landau oscillators have been fully characterized in [21, 22], a systematic analysis for networks with more than two oscillators remains largely unexplored. Focusing on general ring topologies, we analyze the Hopf bifurcation structure of the networked system and show that synchronized oscillations can also arise when amplitude dynamics are explicitly taken into account.

We emphasize that for general network topologies, the parameter μ must be sufficiently large to guarantee synchronization, and we provide explicit sufficient conditions on the initial data (see, Theorem 3.1 and Theorem 3.2). In contrast, when μ is close to zero, a restriction to highly symmetric—yet still broadly representative—ring networks allows for a block-diagonalization of the linearized system. This structural simplification enables a precise analysis of Hopf bifurcation points

and ensures the emergence of synchronized states at criticality (see, Theorem 4.1-Theorem 4.2).

2. MODEL AND SYNCHRONIZATION

We consider an ensemble of N diffusively coupled Stuart–Landau oscillators governed by

$$(2.1) \quad \dot{z}_j = (\mu + i\omega_j)z_j - |z_j|^2 z_j + c \sum_{k=1}^N a_{jk} (z_k - z_j), \quad j = 1, \dots, N.$$

Equation (2.1) preserves the global $U(1)$ phase-shift symmetry and couples the Hopf normal form to network diffusion. Writing polar coordinates $z_j = r_j e^{i\theta_j}$ (for $r_j > 0$), yields

$$(2.2) \quad \begin{cases} \dot{r}_j = (\mu - r_j^2)r_j + c \sum_{k=1}^N a_{jk} (r_k \cos(\theta_k - \theta_j) - r_j), \\ \dot{\theta}_j = \omega_j + c \sum_{k=1}^N a_{jk} \frac{r_k}{r_j} \sin(\theta_k - \theta_j). \end{cases}$$

Remark 2.1. We emphasize that whenever (2.2) is well-defined, i.e., whenever

$$r_j(t) > 0 \quad \text{for all } j \in \{1, \dots, N\} \text{ and for all } t > 0,$$

the system (2.2) is equivalent to the original system (2.1).

Remark 2.2 (Phases and unwrapping). Throughout, we regard θ_j as an *unwrapped* angle, i.e. a continuous map $\theta_j : [0, \infty) \rightarrow \mathbb{R}$ chosen on any interval where $r_j(t) > 0$ and satisfying $e^{i\theta_j(t)} = z_j(t)/r_j(t)$. Accordingly, phase differences $\theta_k - \theta_j$ in (2.2) are taken in \mathbb{R} . When a modulo- 2π notion is intended we explicitly use the circular distance

$$\text{dist}_{\mathbb{S}^1}(\alpha, \beta) = \min_{m \in \mathbb{Z}} |\alpha - \beta + 2\pi m| \in [0, \pi].$$

The evolution (2.2) is invariant under $\theta_j \mapsto \theta_j + 2\pi m_j$, so wrapped and unwrapped conventions are dynamically equivalent as long as $r_j > 0$. If some $r_j(t)$ reaches 0, the angle θ_j is undefined; statements that involve θ_j are understood on intervals where $r_j > 0$, or else via the complex formulation (2.1). In particular, to avoid the division by r_j in (2.2), we either assume an anti-amplitude-death condition after some time (e.g. $\inf_{t \geq T} r_j(t) > 0$ for all j) or carry out arguments directly in the complex coordinates.

Parameters and standing assumptions.

- **Local dynamics.** $\mu > 0$ is the Hopf parameter. For an uncoupled unit ($c = 0$) the origin is unstable and there is a stable limit cycle of radius $\sqrt{\mu}$ with natural frequency ω_j . The cubic coefficient has been non-dimensionalized to 1.
- **Frequencies.** $\omega_j \in \mathbb{R}$ denotes the natural frequency of node j . The identical frequency refers to $\omega_j \equiv \omega$, in which one may, if convenient, pass to a rotating frame to set the common frequency to zero.
- **Coupling strength.** $c \geq 0$ scales the diffusive interaction. We keep c separate from the topology so that $A = [a_{jk}]$ encodes structure while c is a scalar control.

- **Unweighted, undirected, connected adjacency matrix.** We work on a simple undirected graph $G = (V, E)$ with $V = \{1, \dots, N\}$ and adjacency matrix $A = [a_{jk}]$ satisfying:

- (i) **Binary edges:** $a_{jk} \in \{0, 1\}$ for all j, k , and $a_{jj} = 0$ (no self-loops).
- (ii) **Symmetry (undirected):** $a_{jk} = a_{kj}$ for all j, k .
- (iii) **Connectivity:** G is connected; equivalently, with $D = \text{diag}(d_1, \dots, d_N)$, $d_j = \sum_k a_{jk}$, and the combinatorial Laplacian,

$$(2.3) \quad L = D - A,$$

we have $\ker L = \text{span}\{\mathbf{1}\}$; that is, the algebraic connectivity satisfies $\lambda_2(L) > 0$, where $\mathbf{1} := (1, \dots, 1)^\top$.

With this notation the coupling can be written compactly as

$$(2.4) \quad c \sum_{k=1}^N a_{jk} (z_k - z_j) = -c \sum_{k=1}^N L_{jk} z_k,$$

so that diffusion acts along Laplacian modes.

Remark 2.3. The system is equivariant under the global phase shift $z_j \mapsto e^{i\varphi} z_j$, hence phase locking is understood modulo a common rotation. In polar coordinates the angle θ_j is defined only for $r_j > 0$; statements that involve θ_j are interpreted on the set where r_j stays positive (or by continuity through the complex form). All symbols are dimensionless unless otherwise stated.

Remark 2.4. For the unweighted, undirected complete graph K_N with $V = \{1, \dots, N\}$ and adjacency matrix A , we have

$$L = D - A = (N - 1)I - (J - I) = NI - J,$$

where I is identity matrix and $J_{jk} = 1$ for all $j, k \in \{1, \dots, N\}$. Therefore, we have

$$0 = \lambda_1(L) < \lambda_2(L) = \dots = \lambda_N(L) = N.$$

The primary objective of this paper is to identify and classify sufficient conditions that guarantee exponential frequency-amplitude synchronization for networks with nonidentical natural frequencies and uniform exponential complete synchronization in the identical natural frequency case. For the convenience of subsequent analysis, we introduce several notations and auxiliary functions below. Let

$$z(t) := (z_1(t), \dots, z_N(t)) \in \mathbb{C}^N,$$

$$r(t) := (r_1(t), \dots, r_N(t)) \in \mathbb{R}_{\geq 0}^N, \quad \theta(t) := (\theta_1(t), \dots, \theta_N(t)) \in \mathbb{R}^N,$$

for $t \geq 0$, and let

$$\Omega := (\omega_1, \dots, \omega_N) \in \mathbb{R}^N$$

denote the vector of natural frequencies. We define the mean quantities by

$$\bar{z}(t) := \frac{1}{N} \sum_{j=1}^N z_j(t), \quad \bar{r}(t) := \frac{1}{N} \sum_{j=1}^N r_j(t), \quad \bar{\theta}(t) := \frac{1}{N} \sum_{j=1}^N \theta_j(t), \quad \bar{\omega} := \frac{1}{N} \sum_{j=1}^N \omega_j.$$

Throughout, we consider solutions $z(t)$ of the original Stuart–Landau network (2.1). In fact, under suitable initial data and coupling strength, each amplitude remains strictly positive for all $t \geq 0$; that is, $r_j(t) = |z_j(t)| > 0$ for all $j \in \{1, \dots, N\}$ (see Lemma 2.2). Hence the polar representation $z_j(t) = r_j(t)e^{i\theta_j(t)}$

is globally well-defined, and system (2.2) is equivalent to (2.1). Under this anti-amplitude-death condition, we introduce the following notions of synchronization.

Definition 2.1 (Frequency-amplitude synchronization). We say that the network achieves *frequency-amplitude synchronization* if

$$\lim_{t \rightarrow \infty} |r_j(t) - r_k(t)| = 0, \quad \lim_{t \rightarrow \infty} |\dot{r}_j(t) - \dot{r}_k(t)| = 0, \quad \lim_{t \rightarrow \infty} |\dot{\theta}_j(t) - \dot{\theta}_k(t)| = 0,$$

for all $j, k \in \{1, \dots, N\}$. If the above convergence occurs at an exponential rate, we say that the system achieves *exponential frequency-amplitude synchronization*.

Definition 2.2 (Complete synchronization). If, in addition to frequency-amplitude synchronization, the phases satisfy

$$\lim_{t \rightarrow \infty} \text{dist}_{\mathbb{S}^1}(\theta_j(t), \theta_k(t)) = 0, \quad \forall j, k \in \{1, \dots, N\},$$

then the network is said to achieve *complete synchronization*. If the convergence is exponential, we refer to it as *exponential complete synchronization*.

Remark 2.5. A necessary condition for complete synchronization is that all oscillators share the same natural frequency, namely

$$\omega_j = \omega, \quad j = 1, 2, \dots, N.$$

When this condition holds, the oscillators are said to be identical.

To the best of our knowledge, sufficient conditions for avoiding amplitude death have thus far been formulated only in an intuitive manner. We present several properties of system (2.1), stated as lemmas below.

Lemma 2.1 (Instability of Complete Amplitude Death). *If $\mu > c \lambda_{\max}(L)$, then the complete amplitude death equilibrium $z = 0$ of (2.1) is unstable.*

Proof. Linearizing (2.1) around $z = 0$ and recalling (2.3), we obtain

$$\dot{z} = \mathcal{L}z, \text{ where } \mathcal{L} = \mu I - cL + i \text{diag}(\omega_1, \dots, \omega_N).$$

Note that

$$\lambda_{\min}(\mu I - cL) \leq \Re \lambda(\mathcal{L}) \leq \lambda_{\max}(\mu I - cL).$$

Since

$$\lambda_{\min}(\mu I - cL) = \mu - \lambda_{\max}(L) > 0,$$

it follows that $\Re \lambda(\mathcal{L}) > 0$. Hence, $z = 0$ is unstable. \square

However, guaranteeing that each $|z_j| = r_j$ remains strictly nonzero throughout the evolution requires a more refined description. In fact, the absence of amplitude death in every component of the system (so that (2.2) remains well-defined) depends not only on the system parameters but also on the initial conditions. We present sufficient conditions ensuring the persistence of nonvanishing amplitudes below.

Lemma 2.2 (Persistence of Nonvanishing Amplitudes). *Assume that*

$$(2.5) \quad c < c^* := \frac{2\mu}{3\sqrt{3N} \lambda_{\max}(L)}.$$

Suppose the initial conditions satisfy

$$(2.6) \quad \sum_{j=1}^N r_j^2(0) \leq N\mu, \quad r_j(0) > r^* := \min \left\{ x > 0 : \mu x - x^3 = c\sqrt{N\mu} \lambda_{\max}(L) \right\},$$

for all $j = 1, \dots, N$. Then the solution of (2.2) exists globally, and there exists $T > 0$ such that for all $t > T$,

$$(2.7) \quad r^* < r_j(t) < \sqrt{\mu}, \quad \forall j = 1, \dots, N.$$

In particular, each component of $r(t)$ remains strictly positive for all $t > 0$, so no amplitude death occurs, and (2.2) is equivalent to (2.1).

We provide the proof of Lemma 2.2 in Appendix A for completeness. We note in passing that if $\sum_{j=1}^N r_j^2(0) > N\mu$, a condition analogous to (2.6) likewise guarantees the persistence of positive amplitudes. As the argument is essentially the same, we omit the details.

Next, we consider the network (2.1) with identical natural frequencies, i.e. $\omega_j \equiv 0$ for all $j = 1, \dots, N$. To quantify the total squared frequency of the oscillators, we introduce the energy-type functional

$$(2.8) \quad \mathcal{H}(t) := \int_0^t \sum_{j=1}^N \left(|\dot{r}_j(s)|^2 + |r_j(s)\dot{\theta}_j(s)|^2 \right) ds.$$

Multiplying the first equation of (2.2) by \dot{r}_j and the second equation by $r_j^2\dot{\theta}_j$, summing over $j = 1, \dots, N$, and integrating in time over $[0, t]$, we obtain

$$(2.9) \quad \mathcal{H}(t) = \int_0^t \mathcal{I}(s) ds + \int_0^t \mathcal{II}(s) ds,$$

where

$$(2.10) \quad \mathcal{I}(t) := \sum_{j=1}^N \left((\mu - r_j^2) r_j - c \sum_{k=1}^N a_{jk} \right) \dot{r}_j,$$

$$(2.11) \quad \mathcal{II}(t) := c \sum_{j=1}^N \sum_{k=1}^N a_{jk} \left(r_k \dot{r}_j \cos(\theta_k - \theta_j) + r_k r_j \sin(\theta_k - \theta_j) \dot{\theta}_j \right).$$

Exploiting the symmetry of a_{jk} , \mathcal{II} can be rewritten as

$$(2.12) \quad \mathcal{II}(t) = \frac{c}{2} \frac{d}{dt} \sum_{j=1}^N \sum_{k=1}^N \left(a_{jk} r_j r_k \cos(\theta_k(t) - \theta_j(t)) \right).$$

If r_j remains bounded, then the right-hand side of (2.9) is bounded by a constant independent of time. Moreover, from (2.2) one checks that $\mathcal{H}(t)$ is uniformly continuous. Consequently,

$$\lim_{t \rightarrow \infty} \sum_{j=1}^N \left(|\dot{r}_j(t)|^2 + |r_j(t)\dot{\theta}_j(t)|^2 \right) = 0.$$

This yields the following lemma.

Lemma 2.3 (Energy Functional). *Consider the network (2.1) with $\omega_j \equiv 0$ for all $j = 1, \dots, N$. Let $(r(t), \theta(t))$ be a solution of (2.2) such that $0 < r_j(t) < l$ for some constants $l > 0$ and all $j = 1, \dots, N$. Then*

$$\lim_{t \rightarrow \infty} \dot{r}_j = 0 \quad \text{and} \quad \lim_{t \rightarrow \infty} \dot{\theta}_j = 0.$$

3. SYNCHRONIZATION FOR GENERAL NETWORK TOPOLOGIES

In this section, we consider a general network topology given by a simple, undirected, and connected graph $G = (V, E)$, $V = \{1, \dots, N\}$. The associated adjacency matrix $A = [a_{jk}]$ satisfies $a_{jk} \in \{0, 1\}$, $a_{jj} = 0$, $a_{jk} = a_{kj}$ for all $j, k \in V$.

Theorem 3.1 (Topology-Robust Synchronization). *Let (2.5) and (2.6) hold. Assume that $\omega_j = \omega \in \mathbb{R}$ for all $j \in \{1, \dots, N\}$. Let z be a solution of (2.1) with initial condition satisfying*

$$0 < \theta_j(0) < \pi, \quad \forall j \in \{1, \dots, N\}.$$

Then the solution exists globally and the network achieves complete synchronization. More precisely, there exists a phase $\vartheta_0 \in (0, \pi)$ such that

$$(3.1) \quad \begin{aligned} \lim_{t \rightarrow \infty} r_j(t) &= \sqrt{\mu}, & \lim_{t \rightarrow \infty} |\dot{r}_j(t) - \dot{r}_k(t)| &= 0, \\ \lim_{t \rightarrow \infty} |\dot{\theta}_j(t) - \dot{\theta}_k(t)| &= 0, & \lim_{t \rightarrow \infty} \text{dist}_{\mathbb{S}^1}(\theta_j(t), \vartheta_0) &= 0, \end{aligned}$$

for all $j, k \in \{1, \dots, N\}$. Moreover, both limits above are achieved at an exponential rate; hence the network attains exponential complete synchronization.

Proof. By Lemma 2.2, we may restrict attention to system (2.2). Passing to the co-rotating frame $\theta_j \mapsto \theta_j - \omega t$ gives

$$(3.2) \quad \begin{cases} \dot{r}_j = (\mu - r_j^2)r_j + c \sum_{k=1}^N a_{jk}(r_k \cos(\theta_k - \theta_j) - r_j), \\ \dot{\theta}_j = c \sum_{k=1}^N a_{jk} \frac{r_k}{r_j} \sin(\theta_k - \theta_j). \end{cases}$$

At each $t > 0$, let $\sigma(t)$ be the permutation that orders the phases:

$$\theta_{(1)}(t) \leq \theta_{(2)}(t) \leq \dots \leq \theta_{(N)}(t), \quad \theta_{(j)}(t) := \theta_{\sigma_j(t)}(t),$$

and define

$$\theta_{\min}(t) = \theta_{(1)}(t), \quad \theta_{\max}(t) = \theta_{(N)}(t).$$

Since $\theta(t)$ is analytic, any two trajectories can coincide only finitely many times on a bounded interval, so θ_{\min} and θ_{\max} are piecewise C^∞ in t .

Step 1: Invariant phase interval. We first show

$$(3.3) \quad 0 < \theta_{\min}(t) \leq \theta_{\max}(t) < \pi, \quad t \geq 0.$$

Suppose, for contradiction, that θ_{\max} reaches π or θ_{\min} reaches 0 at the first time $T_0 > 0$. Without loss of generality, assume $\theta_{\max}(T_0) = \pi$ and $0 < \theta_{\min}(t) \leq \theta_{\max}(t) < \pi$ for $t < T_0$. On each interval where θ_{\max} coincides with some θ_j , differentiating (3.2) yields

$$\dot{\theta}_j = c \sum_{k=1}^N a_{jk} \frac{r_k}{r_j} \sin(\theta_k - \theta_j) \leq 0,$$

since $0 < \theta_k \leq \theta_j < \pi$. Hence $\theta_{\max}(t)$ is nonincreasing, and by induction with $\theta_{\max}(0) < \pi$, one obtains $\theta_{\max}(T_0) < \pi$, a contradiction. Therefore (3.3) holds for all $t \geq 0$.

Step 2: Asymptotic alignment. By monotonicity, the limits

$$\theta_{\max}(t) \downarrow \phi_M, \quad \theta_{\min}(t) \uparrow \phi_m, \quad 0 < \phi_m \leq \phi_M < \pi$$

exist. Lemmas 2.2 and 2.3 imply $|\dot{\theta}_j| \rightarrow 0$ for all j . Selecting $t_n = n \in \mathbb{N}$, the sequence $\{(r(t_n), \theta(t_n))\}$ is bounded in \mathbb{R}^{2N} by (2.7) and (3.3). By Bolzano–Weierstrass, it has a convergent subsequence $(r^{(1)}(t_n), \theta^{(1)}(t_n))$. Passing to the limit $t_n \rightarrow \infty$ in the second equation of (3.2) yields $\phi_m = \phi_M$, proving that all oscillators attain phase synchronization.

Step 3: Amplitude saturation. Let j_* be such that $r_{j_*}(t) = \min_j r_j(t)$. Since $\cos(\theta_k - \theta_{j_*}) \rightarrow 1$ as $t \rightarrow \infty$, we have, for large t ,

$$r_k(t) \cos(\theta_k - \theta_{j_*}) \geq r_{j_*}(t) \cos(\theta_k - \theta_{j_*}).$$

Substituting into (3.2) gives

$$\dot{r}_{j_*} \geq (\mu - \mathfrak{R}(t) - r_{j_*}^2) r_{j_*}, \quad \mathfrak{R}(t) := c \sum_{k=1}^N a_{j_*k} (1 - \cos(\theta_k - \theta_{j_*})) \geq 0.$$

As $\mathfrak{R}(t)$ tends to zero, we have $\dot{r}_{j_*} > 0$ whenever $0 < r_{j_*} < \sqrt{\mu - \mathfrak{R}(t)}$, implying $\lim_{t \rightarrow \infty} r_{j_*}(t) = \sqrt{\mu}$. Combining with Lemma 2.2 (cf. (2.7)) completes the proof. \square

Theorem 3.2. *Assume that $\omega_j = \omega \in \mathbb{R}$ for all $j \in \{1, \dots, N\}$ and*

$$(3.4) \quad \mu > c d_{\max} := c \max_{1 \leq j \leq N} \left(\sum_{k=1}^N a_{jk} \right).$$

Let z be a solution of (2.1) with initial condition satisfying

$$0 < \theta_j(0) < \frac{\pi}{2} \quad \forall j \in \{1, \dots, N\}.$$

Then, there exist a phase $\vartheta^ \in (0, \frac{\pi}{2})$ such that*

$$(3.5) \quad \begin{aligned} \lim_{t \rightarrow \infty} r_j(t) &= \sqrt{\mu}, & \lim_{t \rightarrow \infty} |\dot{r}_j(t) - \dot{r}_k(t)| &= 0, \\ \lim_{t \rightarrow \infty} |\dot{\theta}_j(t) - \dot{\theta}_k(t)| &= 0, & \lim_{t \rightarrow \infty} \text{dist}_{\mathbb{S}^1}(\theta_j(t), \vartheta^*) &= 0, \end{aligned}$$

for all $j, k \in \{1, \dots, N\}$. Moreover, both limits above are achieved at an exponential rate; hence the network attains exponential complete synchronization.

Proof. Following the argument of Step 1 in the previous proof, we first establish

$$(3.6) \quad 0 < \theta_{\min}(t) \leq \theta_{\max}(t) < \frac{\pi}{2}, \quad t \geq 0.$$

Hence $r_j(t) > 0$ for all $t > 0$. Indeed, letting $r_{j_*}(t) = \min_{1 \leq j \leq N} r_j(t)$, we compute

$$\begin{aligned} \dot{r}_{j_*} &= (\mu - r_{j_*}^2) r_{j_*} + c \sum_{k=1}^N a_{j_*k} (r_k \cos(\theta_k - \theta_{j_*}) - r_{j_*}) \\ &\geq (\mu - c d_{\max} - r_{j_*}^2) r_{j_*} > 0, \end{aligned}$$

whenever $r_{j*}(t) \in (0, \sqrt{\mu - c d_{\max}})$. Combining this with (A.5) yields

$$\min\{r_{j*}(0), \sqrt{\mu - c d_{\max}}\} \leq r_{j*}(t) < \sqrt{\mu}, \quad t > 0.$$

By Lemma 2.3, we further have

$$\lim_{t \rightarrow \infty} \dot{r}_j(t) = 0, \quad \lim_{t \rightarrow \infty} \dot{\theta}_j(t) = 0.$$

Finally, invoking the same reasoning as in Steps 2 and 3 of the previous proof, we conclude that all oscillators converge to a common phase and amplitude, completing the proof of Theorem 3.2. \square

4. HOPF BIFURCATION ANALYSIS IN SYMMETRIC NETWORKS

While the results in Section 3 describe synchronization under general network topologies, they do not address the critical regime $\mu = 0$. In this section, we focus on a broad class of ring-symmetric coupling structures and employ a Hopf bifurcation analysis to establish the existence of synchronized states.

Our analysis has two components. First, we restrict system (4.1) to the synchronous manifold and show that a Hopf bifurcation occurs at $\mu = 0$, giving rise to a branch of synchronous periodic solutions. Second, we return to the full system and study the linearization at the origin. Using the block-circulant structure induced by the ring symmetry and its Fourier diagonalization, the Jacobian matrix decomposes into N independent 2×2 blocks. This decomposition yields additional critical parameter values associated with non-synchronous modes and clarifies the symmetry-induced multiplicities that may lead to degeneracies. Explicit formulas for the blocks M_j are derived later in this section and summarized in Appendix C.

Writing $z_j = x_j + iy_j$ in (2.1), we obtain

$$(4.1) \quad \begin{cases} \dot{x}_j = \mu x_j - \omega y_j - x_j(x_j^2 + y_j^2) + c \sum_{k=1}^N a_{jk}(x_k - x_j), \\ \dot{y}_j = \omega x_j + \mu y_j - y_j(x_j^2 + y_j^2) + c \sum_{k=1}^N a_{jk}(y_k - y_j), \end{cases}$$

for $j = 1, 2, \dots, N$.

We consider the s -nearest-neighbor ring coupling defined by

$$(4.2) \quad a_{jk} = \begin{cases} 1, & 1 \leq |j - k|_N \leq s, \\ 0, & \text{otherwise,} \end{cases}$$

where

$$|j - k|_N := \min\{|j - k|, N - |j - k|\}$$

denotes the distance on the ring under the closest distance convention [40].

Remark 4.1.

(a) The coupling (4.2) can be equivalently written as

$$a_{jk} = \begin{cases} 1, & k = j \pm \ell \pmod{N}, \quad \ell = 1, 2, \dots, s, \\ 0, & \text{otherwise.} \end{cases}$$

(b) When $s = 1$, (4.2) reduces to the nearest-neighbor ring coupling, for which

$$a_{jk} = \begin{cases} 1, & k = j \pm 1 \pmod{N}, \\ 0, & \text{otherwise.} \end{cases}$$

(c) When

$$s = \begin{cases} N/2, & N \text{ even,} \\ (N-1)/2, & N \text{ odd,} \end{cases}$$

the coupling (4.2) becomes all-to-all without self-coupling, namely,

$$a_{jk} = \begin{cases} 1, & k \neq j, \\ 0, & k = j. \end{cases}$$

To study the onset of oscillations, we linearize system (4.1) at the origin. This yields the $2N \times 2N$ Jacobian matrix

$$(4.3) \quad A = \begin{bmatrix} A_1 & A_2 & A_3 & \cdots & A_N \\ A_N & A_1 & A_2 & \cdots & A_{N-1} \\ \vdots & \vdots & & \ddots & \\ A_2 & A_3 & A_4 & \cdots & A_1 \end{bmatrix},$$

where each A_k is a 2×2 matrix. Thus A is a block-circulant matrix of type $(N, 2)$, denoted by $A = \text{bcirc}(A_1, \dots, A_N) \in \mathcal{BC}_{N,2}$ [41].

To exploit this structure, we introduce the discrete Fourier transform.

Definition 4.1. The Fourier matrix of order n is defined by

$$F_n := \frac{1}{\sqrt{n}} [w^{(j-1)(k-1)}]_{j,k=1}^n, \quad \text{where } w = e^{-2\pi i/n}.$$

This matrix is also known as the discrete Fourier transform (DFT) matrix.

Lemma 4.1 (Theorem 5.6.4 [41]). *A matrix $A \in \mathcal{BC}_{m,n}$ if and only if it can be expressed in the form*

$$(4.4) \quad A = (F_m \otimes F_n)^* \text{diag}(M_1, M_2, \dots, M_m) (F_m \otimes F_n),$$

where

$$(4.5) \quad \begin{bmatrix} M_1 \\ M_2 \\ \vdots \\ M_m \end{bmatrix} = (\sqrt{m} F_m \otimes I_n) \begin{bmatrix} B_0 \\ B_1 \\ \vdots \\ B_{m-1} \end{bmatrix}, \quad B_{k-1} = F_n^* A_k F_n, \quad k = 1, 2, \dots, m,$$

and each M_k is a square matrix of order n .

Remark 4.2. Since the Fourier matrices F_m and F_n are unitary (Theorem 2.5.1 [41]), their Kronecker product $F_m \otimes F_n$ is also unitary. Indeed,

$$(F_m \otimes F_n)^* (F_m \otimes F_n) = (F_m^* F_m) \otimes (F_n^* F_n) = I_m \otimes I_n = I_{mn}.$$

Applying Lemma 4.1 to (4.3), the Jacobian matrix is unitarily similar to a block-diagonal matrix consisting of N independent 2×2 blocks M_1, M_2, \dots, M_N . The block M_1 corresponds to the dynamics on the synchronous manifold, whereas the remaining blocks describe non-synchronous dynamics.

To investigate synchronized periodic solutions, we first restrict the dynamics to the synchronous manifold

$$\mathcal{S} := \{x_i = x_j, y_i = y_j : 1 \leq i, j \leq N\}.$$

If $(x_j(t), y_j(t)) \equiv (x(t), y(t))$ for all j , then all coupling terms vanish, and system (4.1) reduces on \mathcal{S} to

$$(4.6) \quad \begin{cases} \dot{x} = \mu x - \omega y - x(x^2 + y^2), \\ \dot{y} = \omega x + \mu y - y(x^2 + y^2). \end{cases}$$

This type of synchronous-manifold reduction has been used, for example, in [42, 43].

Theorem 4.1. *The reduced system (4.6) undergoes a supercritical Hopf bifurcation at $\mu = 0$ and $(x, y) = (0, 0)$. Consequently, system (4.1) admits a branch of synchronous periodic solutions bifurcating from the origin for $\mu > 0$ and μ close to 0, which are asymptotically stable within the synchronous manifold \mathcal{S} in the sense of Definitions 2.1 and 2.2.*

The proof is based on a standard Hopf normal form computation following [44] and is given in Appendix B.

The Hopf bifurcation at $\mu = 0$ established in Theorem 4.1 is associated with the synchronous mode (the block M_1 in the decomposition (4.4)). We now return to the full Jacobian matrix (4.3) to identify additional critical parameter values arising from the remaining blocks.

More precisely, for each $j = 2, 3, \dots, N$, the block M_j has eigenvalues that are purely imaginary at a critical parameter value $\mu = \mu_j$. A direct computation of M_j , carried out later in this section, shows that

$$(4.7) \quad \mu = \mu_j := 2c \left(s - \frac{\sin\left[\frac{s(j-1)\pi}{N}\right] \cos\left[\frac{(s+1)(j-1)\pi}{N}\right]}{\sin\left[\frac{(j-1)\pi}{N}\right]} \right), \quad j = 2, 3, \dots, N.$$

Thus, $\mu = \mu_j$ is a critical parameter value at which the linearization acquires a pair of purely imaginary eigenvalues in the j th non-synchronous mode. Owing to symmetry-induced multiplicities, the associated Hopf critical point may be degenerate and does not, by itself, determine the nonlinear dynamics near the origin. Further details on the derivation and properties of (4.7) are provided at the end of this section.

Proposition 4.1 (Symmetry of the candidates). *Let μ_j be defined by (4.7) for $j = 2, 3, \dots, N$. Then*

$$\mu_j = \mu_{N+2-j}, \quad j = 2, 3, \dots, N.$$

Moreover, in the non-all-to-all case, the following statements hold:

(i) *If N is even and $1 \leq s \leq \frac{N}{2} - 1$, then there is a unique index $j^* = 1 + \frac{N}{2}$ such that $j^* = N + 2 - j^*$. The remaining indices are paired as*

$$\{2, 3, \dots, N\} \setminus \{j^*\} = \bigsqcup_{j=2}^{\frac{N}{2}} \{j, N + 2 - j\}.$$

(ii) If N is odd and $1 \leq s \leq \frac{N-1}{2} - 1$, then the indices $\{2, 3, \dots, N\}$ are partitioned into disjoint pairs

$$\{2, 3, \dots, N\} = \bigsqcup_{j=2}^{\frac{N+1}{2}} \{j, N+2-j\}.$$

In particular, in the all-to-all case, namely $s = \frac{N}{2}$ for even N or $s = \frac{N-1}{2}$ for odd N , the expression (4.7) simplifies to

$$\mu_2 = \mu_3 = \dots = \mu_N = Nc.$$

Proof. Using the identities

$$\sin(\pi - \theta) = \sin \theta, \quad \cos(\pi - \theta) = -\cos \theta,$$

and

$$\sin(s\pi - \theta) = (-1)^{s+1} \sin \theta, \quad \cos((s+1)\pi - \theta) = (-1)^{s+1} \cos \theta,$$

we compute

$$\begin{aligned} \frac{\sin\left[\frac{s(N+1-j)\pi}{N}\right] \cos\left[\frac{(s+1)(N+1-j)\pi}{N}\right]}{\sin\left[\frac{(N+1-j)\pi}{N}\right]} &= \frac{\sin\left[s\pi - \frac{s(j-1)\pi}{N}\right] \cos\left[(s+1)\pi - \frac{(s+1)(j-1)\pi}{N}\right]}{\sin\left[\pi - \frac{(j-1)\pi}{N}\right]} \\ &= \frac{\sin\left[\frac{s(j-1)\pi}{N}\right] \cos\left[\frac{(s+1)(j-1)\pi}{N}\right]}{\sin\left[\frac{(j-1)\pi}{N}\right]}. \end{aligned}$$

Substituting this identity into (4.7) yields $\mu_{N+2-j} = \mu_j$. \square

Proposition 4.2 (Transversality of the critical eigenvalues). *For each $j = 2, 3, \dots, N$, the eigenvalues of the block M_j can be written as*

$$\lambda_j^\pm(\mu) = (\mu - \mu_j) \pm i\omega,$$

where μ_j is given by (4.7). Then

$$\Re \lambda_j^\pm(\mu_j) = 0 \quad \text{and} \quad \Re((\lambda_j^\pm)'(\mu_j)) = 1 \neq 0.$$

Hence, for each $j = 2, 3, \dots, N$, the pair $\lambda_j^\pm(\mu)$ crosses the imaginary axis transversely at $\mu = \mu_j$.

Remark 4.3. Proposition 4.2 provides a transversality condition for each individual mode j . Whether $\mu = \mu_j$ corresponds to a simple Hopf bifurcation further depends on the multiplicity of the critical eigenvalues, that is, on how many blocks M_k satisfy $\mu_k = \mu_j$, as described in Theorem 4.2.

Theorem 4.2 (Additional critical parameter values). *Consider system (4.1) with s -nearest-neighbor ring coupling in the non-all-to-all cases: N is even with $1 \leq s \leq \frac{N}{2} - 1$, or N is odd with $1 \leq s \leq \frac{N-1}{2} - 1$. Besides the Hopf bifurcation at $\mu = 0$ associated with the block M_1 , the system admits additional critical parameter values $\mu = \mu_j$, $j = 2, 3, \dots, N$, at which the Jacobian matrix has purely imaginary eigenvalues $\pm i\omega$ arising from the corresponding blocks M_j .*

The multiplicity of these eigenvalues, and hence whether the corresponding Hopf critical point is simple or degenerate, depends on the parity of N and on symmetry-induced coincidences among the values μ_j .

- (i) If N is even and $j \neq j^* := 1 + \frac{N}{2}$, then j and $N + 2 - j$ form a distinct pair. Consequently, the blocks M_j and M_{N+2-j} simultaneously contribute two pairs of purely imaginary eigenvalues $\pm i\omega$ at $\mu = \mu_j$, and the associated Hopf critical point is not simple.
- (ii) If N is even and $j = j^*$, then j^* is unpaired in the sense that $j^* = N + 2 - j^*$. In this case, the block M_{j^*} contributes a single pair of purely imaginary eigenvalues $\pm i\omega$ at $\mu = \mu_{j^*}$. Whether the corresponding Hopf critical point is simple or degenerate depends on whether there exist indices $k \neq j^*$ such that $\mu_k = \mu_{j^*}$.
- (iii) If N is odd, then for every $j = 2, 3, \dots, N$, the indices j and $N + 2 - j$ form a pair. Hence, at $\mu = \mu_j$, the blocks M_j and M_{N+2-j} simultaneously contribute two pairs of purely imaginary eigenvalues $\pm i\omega$, and all additional Hopf critical points are not simple.

Remark 4.4. Consider the setting of Theorem 4.2 (ii), where N is even and $j^* = 1 + \frac{N}{2}$. If μ_{j^*} is a simple Hopf critical value, namely,

$$\mu_{j^*} \neq \mu_k \quad \text{for all } k \neq j^*,$$

then the criticality at $\mu = \mu_{j^*}$ is generated solely by the block M_{j^*} . In particular, the corresponding critical mode is non-synchronous (i.e., it is not contained in the synchronous manifold \mathcal{S} .) Numerical simulations suggest that a non-synchronous time-dependent branch may emerge near $\mu = \mu_{j^*}$, and that it may display an anti-phase relation: oscillators separated by $N/2$ nodes tend to oscillate with a phase difference close to π . Figure 1 illustrates a degenerate case where the simplicity assumption fails. For $N = 6$ and $s = 2$, we have $j^* = 4$ and $\mu_2 = \mu_4 = \mu_6 = 0.2$, so multiple blocks become critical at the same parameter value and the Hopf critical point is degenerate. In contrast, when N is odd (Figure 2), all additional critical parameter values arise from paired modes, and hence none of associated Hopf critical points is simple. We emphasize that these observations are based on numerical simulations and symmetry considerations. In this work, we do not carry out a rigorous analysis of the existence or stability of non-synchronous branches in the full system.

Proposition 4.3 (Critical parameter values in the all-to-all case). *Consider system (4.1) in the all-to-all coupling case, namely N is even with $s = \frac{N}{2}$, or N is odd with $s = \frac{N-1}{2}$. The block M_1 has eigenvalues*

$$\lambda_1^\pm(\mu) = \mu \pm i\omega,$$

whereas for each $j = 2, 3, \dots, N$ the block M_j has eigenvalues

$$\lambda_j^\pm(\mu) = (\mu - Nc) \pm i\omega.$$

Consequently, $\mu = 0$ yields exactly one pair of purely imaginary eigenvalues $\pm i\omega$, corresponding to a simple Hopf bifurcation associated with the block M_1 . In contrast, at $\mu = Nc$ the linearization has $(N-1)$ pairs of purely imaginary eigenvalues $\pm i\omega$, arising simultaneously from the blocks M_j , $j = 2, 3, \dots, N$, and the corresponding Hopf critical point is highly degenerate.

Remark 4.5. The strong degeneracy at $\mu = Nc$ in Proposition 4.3 is a direct consequence of the maximal symmetry of the all-to-all coupling.

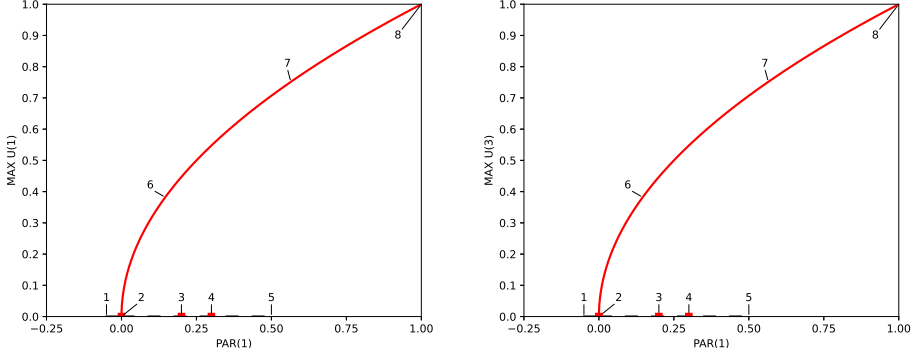


FIGURE 1. Bifurcation diagrams of system (4.1) with $\omega = 1$ and $c = 0.05$ for $N = 6$ and $s = 2$. The horizontal axis is the bifurcation parameter μ , and the vertical axis shows the maxima of x_1 (left) and x_2 (right) along the computed branches. A simple Hopf bifurcation occurs at $\mu = 0$ (point 2). Additional critical parameter values are $\mu_2 = \mu_6 = 0.2$ (point 3) and $\mu_3 = \mu_5 = 0.3$ (point 4); the unpaired index is $j^* = 4$ with $\mu_4 = 0.2$ (point 3).

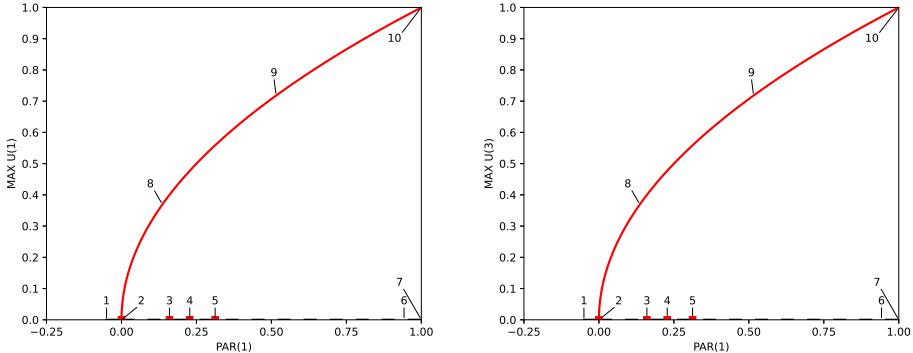


FIGURE 2. Bifurcation diagrams of system (4.1) with $\omega = 1$ and $c = 0.05$ for $N = 7$ and $s = 2$. A simple Hopf bifurcation occurs at $\mu = 0$ (point 2). Additional critical parameter values satisfy $\mu_2 = \mu_7 \approx 0.159903$ (point 3), $\mu_4 = \mu_5 \approx 0.22775$ (point 4), and $\mu_3 = \mu_6 \approx 0.31235$ (point 5). In this odd- N case, all additional critical values correspond to paired modes, and hence none of the associated Hopf critical points is simple.

Up to this point, we have emphasized the bifurcation structure and the symmetry-induced organization of the critical parameter values. In the remainder of this section, we explicitly compute the block matrices M_j and their spectra for different coupling ranges and parities of N . These computations justify the expressions used above and are included for completeness (see Appendix C for details).

By Lemma 4.1 and Remark 4.2, the Jacobian matrix $A \in \mathcal{BC}_{N,2}$ is unitarily similar to $\text{diag}(M_1, M_2, \dots, M_N)$. Consequently,

$$(4.8) \quad \sigma(A) = \bigcup_{j=1}^N \sigma(M_j).$$

We now compute the matrices M_j explicitly. The resulting expressions depend on the parity of N and the coupling range s , and we distinguish the following cases.

Case 1. N is even.

(a) $1 \leq s \leq \frac{N}{2} - 1$ (non-all-to-all coupling). In this case,

$$A_1 = \begin{bmatrix} \mu - 2sc & -\omega \\ \omega & \mu - 2sc \end{bmatrix},$$

and for $\ell = 1, 2, \dots, \frac{N}{2} - 1$,

$$A_{1+\ell} = A_{N-(\ell-1)} = \begin{cases} \begin{bmatrix} c & 0 \\ 0 & c \end{bmatrix}, & \ell = 1, 2, \dots, s, \\ \begin{bmatrix} 0 & 0 \\ 0 & 0 \end{bmatrix}, & \ell = s+1, \dots, \frac{N}{2} - 1. \end{cases}$$

Since N is even, we have $1 + \frac{N}{2} = N - (\frac{N}{2} - 1)$, and thus

$$A_{1+\frac{N}{2}} = \begin{bmatrix} 0 & 0 \\ 0 & 0 \end{bmatrix}.$$

Accordingly,

$$B_0 = \begin{bmatrix} \mu - 2sc & \omega \\ -\omega & \mu - 2sc \end{bmatrix}, \quad B_\ell = B_{N-\ell} = \begin{cases} \begin{bmatrix} c & 0 \\ 0 & c \end{bmatrix}, & \ell = 1, 2, \dots, s, \\ \begin{bmatrix} 0 & 0 \\ 0 & 0 \end{bmatrix}, & \ell = s+1, \dots, \frac{N}{2} - 1, \end{cases}$$

and

$$B_{\frac{N}{2}} = \begin{bmatrix} 0 & 0 \\ 0 & 0 \end{bmatrix}.$$

By (4.5), we obtain

$$M_1 = \begin{bmatrix} \mu & \omega \\ -\omega & \mu \end{bmatrix}$$

and, for $j = 2, 3, \dots, N$,

$$M_j = \begin{bmatrix} \mu - 2c \left(s - \frac{\sin[\frac{s(j-1)\pi}{N}] \cos[\frac{(s+1)(j-1)\pi}{N}]}{\sin[\frac{(j-1)\pi}{N}]} \right) & \omega \\ -\omega & \mu - 2c \left(s - \frac{\sin[\frac{s(j-1)\pi}{N}] \cos[\frac{(s+1)(j-1)\pi}{N}]}{\sin[\frac{(j-1)\pi}{N}]} \right) \end{bmatrix}.$$

The details are given in Appendix C.

Remark 4.6. For any $\theta \in \mathbb{R}$ with $\sin(\frac{\theta}{2}) \neq 0$, the identity

$$\sum_{k=1}^s \cos(k\theta) = \frac{\sin(\frac{s\theta}{2}) \cos(\frac{(s+1)\theta}{2})}{\sin(\frac{\theta}{2})}$$

holds. In particular, for $\theta = \frac{2(j-1)\pi}{N}$ with $j = 2, 3, \dots, N$, we obtain

$$\frac{\sin\left[\frac{s(j-1)\pi}{N}\right] \cos\left[\frac{(s+1)(j-1)\pi}{N}\right]}{\sin\left[\frac{(j-1)\pi}{N}\right]} = \sum_{k=1}^s \cos\left[\frac{2k(j-1)\pi}{N}\right],$$

and hence

$$s - \frac{\sin\left[\frac{s(j-1)\pi}{N}\right] \cos\left[\frac{(s+1)(j-1)\pi}{N}\right]}{\sin\left[\frac{(j-1)\pi}{N}\right]} = \sum_{k=1}^s \left(1 - \cos\left[\frac{2k(j-1)\pi}{N}\right]\right) > 0.$$

(b) $s = \frac{N}{2}$ (all-to-all coupling). In this case,

$$A_1 = \begin{bmatrix} \mu - (N-1)c & -\omega \\ \omega & \mu - (N-1)c \end{bmatrix},$$

and

$$(4.9) \quad A_{1+\ell} = A_{N-(\ell-1)} = A_{1+\frac{N}{2}} = \begin{bmatrix} c & 0 \\ 0 & c \end{bmatrix}, \quad \ell = 1, 2, \dots, \frac{N}{2} - 1.$$

Since $A_{1+\frac{N}{2}} = A_{N-(\frac{N}{2}-1)}$ when N is even, (4.9) is equivalent to

$$A_j = \begin{bmatrix} c & 0 \\ 0 & c \end{bmatrix}, \quad j = 2, 3, \dots, N.$$

A direct application of (4.5) yields

$$(4.10) \quad M_1 = \begin{bmatrix} \mu & \omega \\ -\omega & \mu \end{bmatrix}, \quad M_j = \begin{bmatrix} \mu - Nc & \omega \\ -\omega & \mu - Nc \end{bmatrix}, \quad j = 2, 3, \dots, N.$$

Case 2. N is odd and $1 \leq s \leq \frac{N-1}{2}$. In this case,

$$A_1 = \begin{bmatrix} \mu - 2sc & -\omega \\ \omega & \mu - 2sc \end{bmatrix},$$

and

$$A_{1+\ell} = A_{N-(\ell-1)} = \begin{cases} \begin{bmatrix} c & 0 \\ 0 & c \end{bmatrix}, & \ell = 1, 2, \dots, s, \\ \begin{bmatrix} 0 & 0 \\ 0 & 0 \end{bmatrix}, & \ell = s+1, \dots, \frac{N-1}{2}. \end{cases}$$

By (4.5), we obtain

$$M_1 = \begin{bmatrix} \mu & \omega \\ -\omega & \mu \end{bmatrix}$$

and, for $j = 2, 3, \dots, N$,

$$M_j = \begin{bmatrix} \mu - 2c \left(s - \frac{\sin\left[\frac{s(j-1)\pi}{N}\right] \cos\left[\frac{(s+1)(j-1)\pi}{N}\right]}{\sin\left[\frac{(j-1)\pi}{N}\right]} \right) & \omega \\ -\omega & \mu - 2c \left(s - \frac{\sin\left[\frac{s(j-1)\pi}{N}\right] \cos\left[\frac{(s+1)(j-1)\pi}{N}\right]}{\sin\left[\frac{(j-1)\pi}{N}\right]} \right) \end{bmatrix}.$$

The details are given in Appendix C.

Remark 4.7. In Case 2, when $s = \frac{N-1}{2}$ (equivalently $N = 2s + 1$), the coupling becomes all-to-all. For $j = 2, 3, \dots, N$, we compute

$$\begin{aligned} \frac{\sin\left[\frac{s(j-1)\pi}{N}\right] \cos\left[\frac{(s+1)(j-1)\pi}{N}\right]}{\sin\left[\frac{(j-1)\pi}{N}\right]} &= \frac{1}{2} \frac{\sin\left[\frac{(2s+1)(j-1)\pi}{N}\right] - \sin\left[\frac{(j-1)\pi}{N}\right]}{\sin\left[\frac{(j-1)\pi}{N}\right]} \\ &= \frac{1}{2} \frac{\sin\left[(j-1)\pi\right] - \sin\left[\frac{(j-1)\pi}{N}\right]}{\sin\left[\frac{(j-1)\pi}{N}\right]} = -\frac{1}{2}. \end{aligned}$$

Consequently,

$$\mu - 2c \left(s - \frac{\sin\left[\frac{s(j-1)\pi}{N}\right] \cos\left[\frac{(s+1)(j-1)\pi}{N}\right]}{\sin\left[\frac{(j-1)\pi}{N}\right]} \right) = \mu - 2c \left(\frac{N-1}{2} + \frac{1}{2} \right) = \mu - Nc,$$

and hence

$$M_j = \begin{bmatrix} \mu - Nc & \omega \\ -\omega & \mu - Nc \end{bmatrix}, \quad j = 2, 3, \dots, N,$$

which coincides with (4.10).

APPENDIX A. PERSISTENCE OF NONVANISHING AMPLITUDES

Proof of Lemma 2.2. Define

$$(A.1) \quad R^2(t) := \sum_{j=1}^N |z_j(t)|^2.$$

Recalling (2.1), (2.3), and (2.4), we compute

$$(A.2) \quad \frac{1}{2} \frac{d}{dt} R^2 = \mu R^2 - \sum_{j=1}^N |z_j|^4 - c \bar{z}^\top L z.$$

Since $\bar{z}^\top L z \geq 0$, the Cauchy–Schwarz inequality yields

$$(A.3) \quad \frac{1}{2} \frac{d}{dt} R^2 \leq \mu R^2 - \frac{1}{N} R^4.$$

Hence $R^2(t) < N\mu$ for all $t > 0$.

Next, let j_* be such that $r_{j_*} = \min_{1 \leq j \leq N} r_j$. Differentiating $r_{j_*}^2$ gives

$$\frac{1}{2} \frac{d}{dt} r_{j_*}^2 = \mu r_{j_*}^2 - r_{j_*}^4 - c \Re \left(\sum_k L_{j_*,k} z_k \bar{z}_{j_*} \right).$$

By the Cauchy–Schwarz inequality,

$$\begin{aligned} \left| \Re \left(\sum_k L_{j_*,k} z_k \bar{z}_{j_*} \right) \right| &\leq |z_{j_*}| |(Lz)_{j_*}| \leq r_{j_*} \|Lz\|_2 \leq r_{j_*} \|L\|_2 \|z\|_2 \\ &= r_{j_*} \lambda_{\max}(L) R. \end{aligned}$$

Therefore,

$$(A.4) \quad \frac{1}{2} \frac{d}{dt} r_{j_*}^2 \geq r_{j_*} (\mu r_{j_*} - r_{j_*}^3 - c \sqrt{N\mu} \lambda_{\max}(L)).$$

Together with the initial bound (2.6), this shows that

$$r^* < r_j(t) \quad \forall j = 1, \dots, N \quad \text{and} \quad \forall t > 0$$

Similarly, let j^* be such that $r_{j^*} = \max_{1 \leq j \leq N} r_j$. From the first equation of (2.2) we obtain

$$(A.5) \quad \frac{d}{dt} r_{j^*} = (\mu - r_{j^*}^2) r_{j^*} + c \sum_{k=1}^N A_{j^*k} (r_{j^*} \cos(\theta_k - \theta_{j^*}) - r_{j^*})$$

$$(A.6) \quad \leq (\mu - r_{j^*}^2) r_{j^*}.$$

Hence

$$r_j(t) \leq r_{j^*}(t) < \sqrt{\mu}, \quad \forall j \in \{1, \dots, N\},$$

for all sufficiently large t . This completes the proof. \square

APPENDIX B. PROOF OF THEOREM 4.1

We verify the Hopf bifurcation of the reduced system (4.6) at $\mu = 0$ and determine its direction and stability using the normal form formulas in [44]. For convenience, we denote the components of the vector field by

$$\begin{aligned} F_1(x, y) &:= \mu x - \omega y - x(x^2 + y^2), \\ F_2(x, y) &:= \omega x + \mu y - y(x^2 + y^2). \end{aligned}$$

At $\mu = 0$ and $(x, y) = (0, 0)$, the linearization of system (4.6) admits a pair of purely imaginary eigenvalues $\lambda_1^\pm(0) = \pm i\omega$ and satisfies the transversality condition $\Re((\lambda_1^\pm)'(0)) = 1$. Moreover, system (4.6) is in the standard normal form. Following [44], we introduce the coefficients g_{11} , g_{02} , g_{20} , and G_{21} , which are defined in terms of the second- and third-order partial derivatives of (F_1, F_2) :

$$\begin{aligned} g_{11} &:= \frac{1}{4} \left[\left(\frac{\partial^2 F_1}{\partial x^2} + \frac{\partial^2 F_1}{\partial y^2} \right) + i \left(\frac{\partial^2 F_2}{\partial x^2} + \frac{\partial^2 F_2}{\partial y^2} \right) \right] \\ g_{02} &:= \frac{1}{4} \left[\left(\frac{\partial^2 F_1}{\partial x^2} - \frac{\partial^2 F_1}{\partial y^2} - 2 \frac{\partial^2 F_2}{\partial x \partial y} \right) + i \left(\frac{\partial^2 F_2}{\partial x^2} - \frac{\partial^2 F_2}{\partial y^2} + 2 \frac{\partial^2 F_1}{\partial x \partial y} \right) \right] \\ g_{20} &:= \frac{1}{4} \left[\left(\frac{\partial^2 F_1}{\partial x^2} - \frac{\partial^2 F_1}{\partial y^2} + 2 \frac{\partial^2 F_2}{\partial x \partial y} \right) + i \left(\frac{\partial^2 F_2}{\partial x^2} - \frac{\partial^2 F_2}{\partial y^2} - 2 \frac{\partial^2 F_1}{\partial x \partial y} \right) \right] \\ G_{21} &:= \frac{1}{8} \left[\left(\frac{\partial^3 F_1}{\partial x^3} + \frac{\partial^3 F_1}{\partial x \partial y^2} + \frac{\partial^3 F_2}{\partial x^2 \partial y} + \frac{\partial^3 F_2}{\partial y^3} \right) + i \left(\frac{\partial^3 F_2}{\partial x^3} + \frac{\partial^3 F_2}{\partial x \partial y^2} - \frac{\partial^3 F_1}{\partial x^2 \partial y} - \frac{\partial^3 F_1}{\partial y^3} \right) \right]. \end{aligned}$$

All partial derivatives are evaluated at $\mu = 0$ and $(0, 0)$. Since system (4.6) is two-dimensional, the identity $g_{21} = G_{21}$ holds. A direct computation yields $g_{11} = g_{02} = g_{20} = 0$ and $g_{21} = -2$. Using these coefficients, we compute

$$C_1(0) := \frac{i}{2\omega} (g_{20}g_{11} - 2|g_{11}|^2 - \frac{1}{3}|g_{02}|^2) + \frac{g_{21}}{2} = -1.$$

In particular,

$$\Re(C_1(0)) = -1, \quad \Im(C_1(0)) = 0.$$

Since $\lambda_1^\pm(\mu) = \mu \pm i\omega$, we also have

$$\Re((\lambda_1^\pm)'(0)) = 1, \quad \Im((\lambda_1^\pm)'(0)) = 0.$$

The coefficients in [44] are therefore given by

$$\begin{aligned} p_2 &:= -\frac{\Re(C_1(0))}{\Re((\lambda_1^\pm)'(0))} = 1, \\ \zeta_2 &:= 2\Re(C_1(0)) = -2, \\ T_2 &:= -\frac{1}{\omega} \left(\Im(C_1(0)) + p_2 \Im((\lambda_1^\pm)'(0)) \right) = 0. \end{aligned}$$

Since $p_2 > 0$, the Hopf bifurcation at $\mu = 0$ is supercritical. Moreover, $\zeta_2 < 0$ implies that the bifurcating periodic solutions are asymptotically stable. This completes the proof of Theorem 4.1.

APPENDIX C. DETAILED COMPUTATION OF M_j FOR $j = 1, 2, \dots, N$.

In this appendix, we present the detailed derivation of the block matrices M_j , $j = 1, 2, \dots, N$ appearing in the Fourier diagonalization of the Jacobian matrix. These computations justify the expressions stated in Section 4 and are included for completeness. Recall that the Kronecker product $(\sqrt{N} F_N \otimes I_2)$ takes the explicit form

$$(\sqrt{N} F_N \otimes I_2) = \begin{bmatrix} 1 & 0 & 1 & 0 & 1 & 0 & \cdots & 1 & 0 \\ 0 & 1 & 0 & 1 & 0 & 1 & \cdots & 0 & 1 \\ 1 & 0 & w & 0 & w^2 & 0 & \cdots & w^{N-1} & 0 \\ 0 & 1 & 0 & w & 0 & w^2 & \cdots & 0 & w^{N-1} \\ 1 & 0 & w^2 & 0 & w^4 & 0 & \cdots & w^{2(N-1)} & 0 \\ 0 & 1 & 0 & w^2 & 0 & w^4 & \cdots & 0 & w^{2(N-1)} \\ \vdots & \vdots & \vdots & \vdots & \vdots & \vdots & \ddots & \vdots & \vdots \\ 1 & 0 & w^{N-1} & 0 & w^{2(N-1)} & 0 & \cdots & w^{(N-1)(N-1)} & 0 \\ 0 & 1 & 0 & w^{N-1} & 0 & w^{2(N-1)} & \cdots & 0 & w^{(N-1)(N-1)} \end{bmatrix},$$

where $w = e^{-2\pi i/N}$, consistent with the definition of F_n in Section 4.

Case 1(a): N is even and $1 \leq s \leq \frac{N}{2} - 1$. We write

$$M_1 = \begin{bmatrix} m_1^{11} & m_1^{12} \\ m_1^{21} & m_1^{22} \end{bmatrix} \quad \text{and} \quad M_j = \begin{bmatrix} m_j^{11} & m_j^{12} \\ m_j^{21} & m_j^{22} \end{bmatrix}, \quad j = 2, 3, \dots, N.$$

We compute each entry of M_1 as follows:

$$m_1^{11} = (\mu - 2sc) \cdot 1 + \underbrace{c + \cdots + c}_{s} + \underbrace{0 + \cdots + 0}_{\frac{N}{2} - s - 1} + \underbrace{0}_{1} + \underbrace{0 + \cdots + 0}_{\frac{N}{2} - s - 1} + \underbrace{c + \cdots + c}_{s} = \mu,$$

and a similar computation yields $m_1^{22} = \mu$. Moreover,

$$m_1^{12} = \omega \cdot 1 + \underbrace{0 + \cdots + 0}_{s} + \underbrace{0 + \cdots + 0}_{\frac{N}{2} - s - 1} + \underbrace{0}_{1} + \underbrace{0 + \cdots + 0}_{\frac{N}{2} - s - 1} + \underbrace{0 + \cdots + 0}_{s} = \omega,$$

and a similar computation yields $m_1^{21} = -\omega$.

Similarly, for $j = 2, 3, \dots, N$, we obtain

$$\begin{aligned}
m_j^{11} &= (\mu - 2sc) \cdot 1 + c \cdot \underbrace{(w^{j-1} + w^{2(j-1)} + \dots + w^{s(j-1)})}_s + 0 \cdot \underbrace{(w^{(s+1)(j-1)} + \dots + w^{(\frac{N}{2}-1)(j-1)})}_{\frac{N}{2}-s-1} \\
&\quad + 0 \cdot \underbrace{w^{\frac{N}{2}(j-1)}}_1 + 0 \cdot \underbrace{(w^{[N-(\frac{N}{2}-1)](j-1)} + \dots + w^{[N-(s+1)](j-1)})}_{\frac{N}{2}-s-1} \\
&\quad + c \cdot \underbrace{(w^{(N-s)(j-1)} + \dots + w^{(N-1)(j-1)})}_s \\
&= (\mu - 2sc) + c(w^{j-1} + w^{2(j-1)} + \dots + w^{s(j-1)} + w^{(N-s)(j-1)} + \dots + w^{(N-1)(j-1)}) \\
&= (\mu - 2sc) + c(w^{j-1} + w^{2(j-1)} + \dots + w^{s(j-1)} + w^{-(j-1)} + w^{-2(j-1)} + w^{-s(j-1)}) \\
&= (\mu - 2sc) + c \sum_{k=1}^s \left[w^{k(j-1)} + \frac{1}{w^{k(j-1)}} \right] \\
&= (\mu - 2sc) + c \sum_{k=1}^s 2 \cos \left[\frac{2k(j-1)\pi}{N} \right] \\
&= \mu - 2c \left(s - \frac{\sin[\frac{s(j-1)\pi}{N}] \cos[\frac{(s+1)(j-1)\pi}{N}]}{\sin[\frac{(j-1)\pi}{N}]} \right),
\end{aligned}$$

and a similar computation yields $m_j^{22} = m_j^{11}$. Furthermore,

$$m_j^{12} = \omega \cdot 1 + \underbrace{0 + \dots + 0}_s + \underbrace{0 + \dots + 0}_{\frac{N}{2}-s-1} + \underbrace{0}_1 + \underbrace{0 + \dots + 0}_{\frac{N}{2}-s-1} + \underbrace{0 + \dots + 0}_s = \omega,$$

and a similar computation yields $m_j^{21} = -\omega$.

Case 1(b): N is even and $s = \frac{N}{2}$. We compute each entry of M_1 as follows:

$$m_1^{11} = [\mu - (N-1)c] \cdot 1 + \underbrace{c + c + \dots + c}_{N-1} = \mu,$$

and a similar computation yields $m_1^{22} = \mu$. Moreover,

$$m_1^{12} = \omega \cdot 1 + \underbrace{0 + 0 + \dots + 0}_{N-1} = \omega,$$

and a similar computation yields $m_1^{21} = -\omega$.

Similarly, for $j = 2, 3, \dots, N$, we obtain

$$m_j^{11} = [\mu - (N-1)c] \cdot 1 + c \cdot \underbrace{(w^{j-1} + w^{2(j-1)} + \dots + w^{(N-1)(j-1)})}_{N-1} = \mu - Nc,$$

and a similar computation yields $m_j^{22} = m_j^{11}$. Furthermore,

$$m_j^{12} = \omega \cdot 1 + \underbrace{0 + 0 + \dots + 0}_{N-1} = \omega,$$

and a similar computation yields $m_j^{21} = -\omega$.

Case 2 N is odd and $1 \leq s \leq \frac{N-1}{2}$. We compute each entry of M_1 as follows:

$$m_1^{11} = (\mu - 2sc) \cdot 1 + \underbrace{c + \cdots + c}_{s} + \underbrace{0 + \cdots + 0}_{\frac{N-1}{2}-s} + \underbrace{0 + \cdots + 0}_{\frac{N-1}{2}-s} + \underbrace{c + \cdots + c}_{s} = \mu,$$

and a similar computation yields $m_1^{22} = \mu$. Moreover,

$$m_1^{12} = \omega \cdot 1 + \underbrace{0 + \cdots + 0}_{s} + \underbrace{0 + \cdots + 0}_{\frac{N-1}{2}-s} + \underbrace{0 + \cdots + 0}_{\frac{N-1}{2}-s} + \underbrace{0 + \cdots + 0}_{s} = \omega,$$

and a similar computation yields $m_1^{21} = -\omega$.

Similarly, for $j = 2, 3, \dots, N$, we obtain

$$\begin{aligned} m_j^{11} &= (\mu - 2sc) \cdot 1 + c \cdot \underbrace{(w^{j-1} + w^{2(j-1)} + \cdots + w^{s(j-1)})}_{s} + 0 \cdot \underbrace{(w^{(s+1)(j-1)} + \cdots + w^{(\frac{N-1}{2})(j-1)})}_{\frac{N-1}{2}-s} \\ &\quad + 0 \cdot \underbrace{(w^{[N-(\frac{N-1}{2})](j-1)} + \cdots + w^{[N-(s+1)](j-1)})}_{\frac{N-1}{2}-s} + c \cdot \underbrace{(w^{(N-s)(j-1)} + \cdots + w^{(N-1)(j-1)})}_{s} \\ &= (\mu - 2sc) + c \sum_{k=1}^s \left[w^{k(j-1)} + \frac{1}{w^{k(j-1)}} \right] \\ &= (\mu - 2sc) + c \sum_{k=1}^s 2 \cos \left[\frac{2k(j-1)\pi}{N} \right] \\ &= \mu - 2c \left(s - \frac{\sin \left[\frac{s(j-1)\pi}{N} \right] \cos \left[\frac{(s+1)(j-1)\pi}{N} \right]}{\sin \left[\frac{(j-1)\pi}{N} \right]} \right), \end{aligned}$$

and a similar computation yields $m_j^{22} = m_j^{11}$. Furthermore,

$$m_j^{12} = \omega \cdot 1 + \underbrace{0 + \cdots + 0}_{s} + \underbrace{0 + \cdots + 0}_{\frac{N-1}{2}-s} + \underbrace{0 + \cdots + 0}_{\frac{N-1}{2}-s} + \underbrace{0 + \cdots + 0}_{s} = \omega,$$

and a similar computation yields $m_j^{21} = -\omega$.

ACKNOWLEDGEMENTS

T.-Y. Hsiao is supported by the European Union ERC CONSOLIDATOR GRANT 2023 GUnDHam, Project Number: 101124921. Views and opinions expressed are however those of the authors only and do not necessarily reflect those of the European Union or the European Research Council. Neither the European Union nor the granting authority can be held responsible for them.

REFERENCES

- [1] Kuramoto, Yoshiki, *Self-entrainment of a population of coupled non-linear oscillators*, International Symposium on Mathematical Problems in Theoretical Physics: January 23–29, 1975, Kyoto University, Kyoto/Japan, pp.420–422, 1975.
- [2] Kuramoto, Yoshiki, *Chemical turbulence*, Springer, 1984.
- [3] Hsiao, Ting-Yang and Lo, Yun-Feng and Wang, Winnie *Synchronization in the complexified Kuramoto model*, Nonlinearity, vol. 39, no. 1, pp. 015003, 2025.
- [4] Bronski, Jared C and DeVille, Lee and Jip Park, Moon, *Fully synchronous solutions and the synchronization phase transition for the finite- N Kuramoto model*, Chaos: An Interdisciplinary Journal of Nonlinear Science, vol. 22, no. 3, pp. 033133, 2012.

- [5] Bronski, Jared C and Carty, Thomas and DeVille, Lee, *Configurational stability for the Kuramoto–Sakaguchi model*, Chaos: An Interdisciplinary Journal of Nonlinear Science, vol. 28, no. 10, pp. 103109, 2018.
- [6] Lee, Seungjae and Braun, Lucas and Bönisch, Frieder and Schröder, Malte and Thümler, Moritz and Timme, Marc. *Complexified synchrony*, Chaos: An Interdisciplinary Journal of Nonlinear Science vol. 34, No. 5, 2024.
- [7] Hsiao, Ting-Yang and Lo, Yun-Feng and Zhu, Chengbin *On the Equivalence of Synchronization Definitions in the Kuramoto Flow: A Unified Approach*, arXiv preprint arXiv:2503.19781, 2025.
- [8] Hsiao, Ting-Yang and Lo, Yun-Feng and Zhu, Chengbin *Equivalence of Synchronization States in the Hybrid Kuramoto Flow*, arXiv preprint arXiv:2512.02986, 2025.
- [9] Chen, Shih-Hsin and Hsia, Chun-Hsiung and Hsiao, Ting-Yang, *Complete and Partial Synchronization of Two-Group and Three-Group Kuramoto Oscillators*, SIAM Journal on Applied Dynamical Systems, vol. 23, no. 3, pp. 1720–1765, 2024.
- [10] Bronski, Jared C and DeVille, Lee, *Spectral theory for dynamics on graphs containing attractive and repulsive interactions*, SIAM Journal on Applied Mathematics, vol. 74, no. 1, pp. 83–105, 2014.
- [11] Bronski, Jared C and DeVille, Lee and Ferguson, Timothy, *Graph homology and stability of coupled oscillator networks*, SIAM Journal on Applied Mathematics, vol. 76, no. 3, pp. 1126–1151, 2016.
- [12] Bronski, Jared C and Carty, Thomas and DeVille, Lee, *Synchronization conditions in the Kuramoto model and their relationship to seminorms*, Nonlinearity, vol. 34, no. 8, pp. 5399, 2021.
- [13] Damulewicz, Milena and Ispizua, Juan I and Ceriani, Maria F and Pyza, Elzbieta M, *Communication among photoreceptors and the central clock affects sleep profile*, Frontiers in Physiology, vol. 11, pp. 993, 2020.
- [14] Mirocco, Renato E and Strogatz, Steven H, *Synchronization of pulse-coupled biological oscillators*, SIAM Journal on Applied Mathematics, vol. 50, no. 6, pp. 1645–1662, 1990.
- [15] Strogatz, Steven H and Stewart, Ian, *Coupled oscillators and biological synchronization*, Scientific American, Vol. 269, pp. 102–109, 1993.
- [16] O’Keeffe, Kevin P and Hong, Hyunsuk and Strogatz, Steven H, *Oscillators that sync and swarm*, Nature Communications, vol. 8, pp. 1504, 2017.
- [17] Chen, Kuan-Wei and Shih, Chih-Wen, *Phase-Locked Solutions of a Coupled Pair of Non-identical Oscillators*, Journal of Nonlinear Science, vol. 34, no. 1, pp. 14, 2024.
- [18] Dörfler, Florian and Bullo, Francesco, *Synchronization and transient stability in power networks and nonuniform Kuramoto oscillators*, SIAM Journal on Control and Optimization, vol. 50, no. 3, pp. 1616–1642, 2012.
- [19] Dörfler, Florian and Chertkov, Michael and Bullo, Francesco, *Synchronization in complex oscillator networks and smart grids*, Proceedings of the National Academy of Sciences, vol. 110, no. 6, pp. 2005–2010, 2013.
- [20] Dörfler, Florian and Bullo, Francesco, *Synchronization in complex networks of phase oscillators: A survey*, Automatica, vol. 50, no. 6, pp. 1539–1564, 2014.
- [21] Ermentrout, G Bard, *An adaptive model for synchrony in the firefly *Pteroptyx malaccae**, Journal of Mathematical Biology, vol. 29, no. 6, pp. 571–585, 1991.
- [22] Ermentrout, G Bard and Kopell, Nancy, *Multiple pulse interactions and averaging in systems of coupled neural oscillators*, Journal of Mathematical Biology, vol. 29, no. 3, pp. 195–217, 1991.
- [23] Lohe, MA. *Non-Abelian Kuramoto models and synchronization*, Journal of Physics A: Mathematical and Theoretical vol. 42, No. 39, pp. 395101 2009.
- [24] Bronski, Jared C and Carty, Thomas E and Simpson, Sarah E. *A matrix-valued Kuramoto model*, Journal of Statistical Physics vol. 178, No. 2, pp. 595–624 2020.
- [25] Hsiao, Ting-Yang and Lo, Yun-Feng and Wang, Winnie, *Synchronization in the quaternionic Kuramoto model*, arXiv preprint arXiv:2309.01893, 2023.
- [26] DeVille, Lee. *Synchronization and stability for quantum Kuramoto*, Journal of Statistical Physics vol. 174, No. 1, pp. 160–187 2019.
- [27] Strogatz, Steven H, *Sync: How order emerges from chaos in the universe, nature, and daily life*, Hachette UK, 2012.

- [28] Rodrigues, Francisco A and Peron, Thomas K DM and Ji, Peng and Kurths, Jürgen. *The Kuramoto model in complex networks*, Physics Reports, vol. 610, pp. 1–98 2016.
- [29] Watanabe, Shinya and Strogatz, Steven H. *Constants of motion for superconducting Josephson arrays*, Physica D: Nonlinear Phenomena vol. 74, No. 3-4, pp. 197–253 1994.
- [30] Dai, Jia-Yuan and Fiedler, Bernold and López-Nieto, Alejandro. *Transient rebellions in the Kuramoto oscillator: Morse-Smale structural stability and connection graphs of finite 2-shift type* arXiv preprint arXiv:2512.02937 2025.
- [31] Ha, Seung-Yeal and Kang, Moon-Jin and Lattanzio, Corrado and Rubino, Bruno. *A class of interacting particle systems on the infinite cylinder with flocking phenomena*, Mathematical Models and Methods in Applied Sciences vol. 22, No. 07, pp. 1250008 2012.
- [32] Thümler, Moritz and Srinivas, Shesha GM and Schröder, Malte and Timme, Marc. *Synchrony for weak coupling in the complexified Kuramoto model*, Physical Review Letters vol. 130, No. 18, pp. 187201 2023.
- [33] Andronov, Aleksandr Aleksandrovich. *Les cycles limites de Poincaré et la théorie des oscillations auto-entretenues*, Uspekhi Fizicheskikh Nauk vol. 93, No. 2, pp. 329–331 1967.
- [34] Landau, Lev D. *On the problem of turbulence*, booktitle: Dokl. Akad. Nauk USSR vol. 44, pp. 311 1944.
- [35] Stuart, John Trevor. *On the non-linear mechanics of wave disturbances in stable and unstable parallel flows Part 1. The basic behaviour in plane Poiseuille flow*, Journal of Fluid Mechanics vol. 9, No. 3, pp. 353–370 1960.
- [36] Hopf, Eberhard. *Abzweigung einer periodischen Lösung von einer*, Selected Works of Eberhard Hopf with Commentaries: With Commentaries vol. 17, pp. 91 2002.
- [37] Aronson, Donald G and Ermentrout, G Bard and Kopell, Nancy. *Amplitude response of coupled oscillators*, Physica D: Nonlinear Phenomena vol. 41, No. 3, pp. 403–449 1990.
- [38] Nakao, Hiroya. *Phase reduction approach to synchronisation of nonlinear oscillators*, Contemporary Physics vol. 57, No. 2, pp. 188–214 2016.
- [39] Bick, Christian and Böhle, Tobias and Kuehn, Christian. *Higher-order network interactions through phase reduction for oscillators with phase-dependent amplitude*, Journal of Nonlinear Science vol. 34, No. 4, pp. 77 2024.
- [40] Gupta, Shamik and Campa, Alessandro and Ruffo, Stefano, *Kuramoto model of synchronization: Équilibrium and nonequilibrium aspects*, Journal of Statistical Mechanics: Theory and Experiment, vol. 2014, no. 8, pp. R08001, 2014.
- [41] Davis, Philip J. *Circulant Matrices*. New York: Wiley-Interscience 1979.
- [42] Chen, Kuan-Wei and Liao, Kang-Ling and Shih, Chih-Wen. *The kinetics in mathematical models on segmentation clock genes in zebrafish*, Journal of Mathematical Biology vol. 76, No. 1–2, pp. 97–150, 2018.
- [43] Chen, Kuan-Wei and Shih, Chih-Wen. *Collective oscillations in coupled-cell systems*, Bulletin of Mathematical Biology vol. 83, No. 6, article 62, 2021.
- [44] Hassard, Brian D. and Kazarinoff, Nicholas D. and Wan, Yieh-Hei, *Theory and Applications of Hopf Bifurcation*, London Mathematical Society Lecture Note Series, vol. 41, Cambridge University Press, Cambridge, 1981.